SLAC-PUB-7734
January 1998

Review of Coherent Effects in *B* and Φ Factories

S. Heifets

Stanford Linear Accelerator Center
Stanford University, Stanford, CA 94309

Presented at the 14th Advanced ICFA Beam Dynamics Workshop: Beam Dynamics Issues for E+ E- Factories (ICFA 97), Frascati, Italy, October 20-26, 1997

Work supported by Department of Energy contract DE–AC03–76SF00515.

INTRODUCTION

This talk reviews instabilities which may be relevant to the storage rings under construction and in commissioning such as Φ -factory in Frascati, and the B-factories at SLAC and KEK. For this reason, I don't consider effects specific mostly for proton machines. Beam-beam effects are also not included because today these effects look like a somewhat distant future for the Φ- and B-factories, assumption that may become wrong very quickly. Personal interest and limited knowledge of the author also defined selected topics.

It has been known for more than 30 years that interaction of the beam with environment can cause beam instabilities. Until recently, impedances and wake fields were associated with resistivity and variations of the beam pipe geometry. In addition, interaction with other(foreign) particles, existing or produced by the beam such as ions, trapped- or photo-electrons, may become important for multi-bunch beams, causing instabilities with growth rates substantially higher that these caused by geometric wake fields. The main topics of the talk are

1. Impedances
2. Traditional Instabilities: single- and multi-bunch instabilities
3. Effect of Ions
4. New Instabilities

1 Impedances

The sources of impedances are well understood today and vacuum components of new rings are carefully designed to minimize the impedance budget. This become possible, first of all, due to dramatic progress with 2D and 3D computer codes available today such as ABCI, MAFIA, GDFIDL, and others. At the same time, theory provide analytic results for impedances of small components such as holes or pumping slotsy [1]. and smooth tapers [2] which are difficult do deal with in simulations because of large ascpects ratio typical for such components or/and large number of them in the machines.

Trapped modes, observed before experimentally, have been explained theoretically [3] as a result of frequency shift of a propagating mode close to the beam pipe cutoff $k_c = \omega_c/c_0$ due to perturbed boundary of the beam pipe. These mechanism produces trapped modes only by enlargements of the beam pipe. The localization of the mode $L = 1/q$ and the frequency shift $\Delta\omega$ depends on the volume V of the enlargement

$$\frac{\Delta\omega}{\omega} = \frac{q^2}{2k_c^2}, \quad q = \zeta\frac{k_c^2 V}{2S} \tag{1}$$

where S is the beam pipe cross-section area, and ζ is ratio of the field $|H|^2$ at the enlargement to the average $< |H|^2 >$ over the beam pipe cross-section. Trapped modes may exist as well at cutoff frequencies of all propagating modes. giving resonance enhancement of the real part of the impedance [4], see Fig. 1a.

Any slot in the vacuum chamber would cause some leak of the magnetic field lines into the slots and produce trapped modes. These modes may be avoided by squeezing the beam pipe to make the total variation of the volume equal or less than zero.

It was understood that careful design design of some components such as screens of the vacuum ports (which can produce trapped modes) and of interaction region (where

modes may be trapped between masks and crotches) is needed. For a train of bunches with bunch spacing τ_b, it was emphasized that effect of trapped modes may be enhanced if their frequencies are multiples of $\omega\tau_b/2\pi$. Strict control of temperature may be required to avoid these resonances. Similarly, for a periodic array of components the real part of impedance can be enhanced at resonance frequencies corresponding to propagating constants equal to multipoles of $2\pi/d$ where d is the distance between periodic components.

Small variations of the beam pipe can be taken into account by different forms of perturbation theory [5].

Impedance of coherent radiation, modification of the resistive impedance for very short bunches, and impedance of rough surfaces have been discussed recently. For the Φ- and B-factories these effects can be neglected.

Even when the impedances of all components in the ring are known, there is a question whether the total impedance is the sum of the individual impedances of the ring components. The impedance of a periodic structure, which rolls off with frequency as $\omega^{-3/2}$ instead of $\omega^{-1/2}$ behavior of the impedance of a single cell, clearly indicate that interference of the EM waves radiated by individual components may be important. However, in storage rings (SR), with bunches of with rms σ, in a beam pipe with cut-off frequency $k_c = \omega_c/c_0 << 1/\sigma$, the radiation length L, $L \simeq b^2/2\sigma$, is much less than the average spacing between vacuum components. Therefore interference is suppressed and the impedances of components are additive.

Some caution is needed applying these statement to a periodic array of components where real part of impedance can be enhanced at resonance frequencies corresponding to propagating constant equal to multipoles of $2\pi/d$ where d is the distance between periodic components.

With all this in mind, we can construct impedance of the ring as the sum of the narrow and broad band impedances. The first is given by the sum of HOMs of rf cavities, similar contributions may come from HOMs in the BPMs and trapped modes. The broad-band impedance is the sum of resistive wall impedance and, with proper design, mostly inductive impedances of the vacuum components. A small contribution may come from the high-frequency tail of the impedance of rf cavities, which takes into account the difference of the total loss factor of a cavity and the sum of HOM loss factors in the narrow-band impedances.

The main uncertainty comes from the fact that there are too many vacuum chamber components to model them precisely. In many cases, the available information gives loss factors and inductances of individual components. The impedance of all components have to be constructed with these two parameters. There are two approaches to do this: using $Q = 1$ model (Z_Q) or describing longitudinal impedance by the generalized inductance model (Z_L):

$$Z(\omega) = \frac{R_s}{1 - i(\omega/\omega_r - \omega_r/\omega)}, \quad Z(\omega) = -iZ_0\frac{\omega L}{4\pi c_0(1 - i\omega a/c_0)^{3/2}}. \tag{2}$$

The parameter a, related to the roll-off frequency, defines the loss factor.

Both models have two parameters. The choice of one of them depends, mainly, on bunch length and character of the impedance of a typical vacuum component. For a relatively short bunch and a smooth beam pipe, the inductive impedance is preferable in three aspects: it reproduces much better the character of the wake field of components, it

gives correct roll off at high frequencies, and, being normalized at a nominal rms, gives the dependence of the loss factor on σ in better agreement with numerical code then $Q = 1$ model, see Fig.1b.

The uncertainty with broad-band components in the ring may affect modeling of single bunch instabilities, but is a minor problem for rings with long trains of relatively weak bunches, where multi-bunch instabilities are expected to be the main problem.

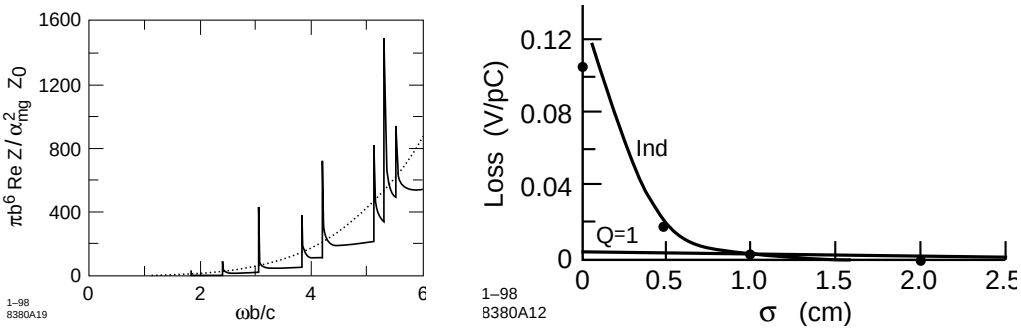

Figure 1: a)On the left: Trapped modes at the beam-pipe cut-offs [4], b) On the right: Loss factor vs σ_l for two impedance models. Dots are ABCI results for a smooth collimator.

2 Conventional Instabilities

The first instability considered in SR is the Robinson instability due to beam loading of rf cavities. The growth rate of the lowest revolution side-bands around the rf frequency depends on the detuning of the cavities, see Fig.2. With proper detuning and direct feedback loops on the cavities (for PEP-II, that includes comb filter feedback) the growth rate of the instability can be reduced to a level where it can be controlled by the bunch-by-bunch longitudinal feedback.

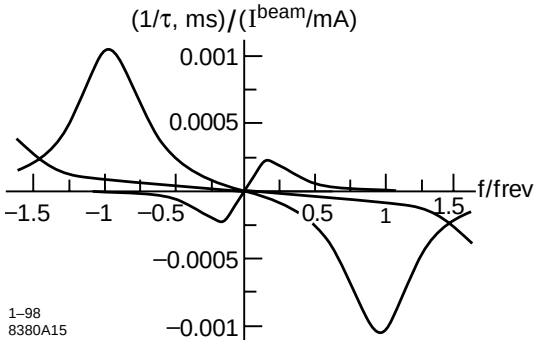

Figure 2: Dependence of the growth rate of Robinson instability for betatron sidebands m=0,-1,-2 around rf on the detuning of rf cavities at PEP-II.

Remaining instabilities are caused by the HOMs of the cavities and all other components in the ring. In the zero-th approximation, the longitudinal and transverse dynamics

can be considered separately. However, this is not always true. For example, transverse HOMs of misaligned rf cavities can be coupled to the longitudinal motion by a finite dispersion giving tune shift [6]

$$\Delta Q_s = -i\frac{Z_\perp e I_b}{2\pi E} x_c D_x. \tag{3}$$

2.1 Single Bunch Instability

At low currents, potential well distortion (PWD) due to the longitudinal wakefield is described by Haiisinski steady-state distribution function [7]

$$\rho(x,p) = \frac{1}{Z}e^{-H}; \quad H(x,p,\tau) = \frac{p^2}{2} + U_{rf} + U_w, \quad \int dxdp\rho = 1, \tag{4}$$

where $p = -\delta/\delta_0$, $x = z/\sigma$, and $\tau = \omega_s t$ are relative momentum offset, position of a particle in respect with bunch centroid, and time in units of zero-current rms σ, δ_0, and synchrotron frequency $\omega_s = \omega_0 Q_s$ respectively. Parameter α is momentum compaction factor, coordinate $x > 0$ in the head of a bunch, $\alpha\delta_0 = \omega_s\sigma/c_0$. Potential $U_{rf} \simeq x^2/2$ is rf potential, and U_w is defined by the wake $W^\delta(z)$ of a point-like particle,

$$\frac{dU_w}{dx} = -\lambda\sigma \int dx'dp'\rho(x',p')W^\delta[\sigma(x'-x)], \quad \lambda = \frac{N_b r_e}{2\pi R\gamma\alpha\delta_0^2}. \tag{5}$$

PWD defines dependence of the rms bunch length, synchronous phase, synchrotron frequency shift, and frequency spread on beam current. The energy spread remains independent of current due to factorized form of Haissinski distribution. Oscillations of a bunch can be described in terms of eigen-modes obtained from linearized Vlasov equation. These results are in quite good agreement with experiment at low currents.

At higher currents, the shift of mode frequencies with current leads to degeneracy. Degenerate modes interact strongly and become unstable. This lead to additional turbulent bunch lengthening. Decay of the unstable modes in single-particle motion leads to heating of the bunch. These phenomena usually referred to as microwave instability. Haissinski distribution is not valid above threshold.

Coupling of radial modes of a given azimuthal mode happens usually first [8], and only at higher currents different azimuthal modes become coupled as well. From this point of view, we can talk about weak and strong microwave instabilities. Oide made a conjecture that the threshold of the weak microwave instability is given approximately by the current for which nonlinearity $d\omega_s/dJ = 0$. Above the threshold of the microwave instability, the instability is inhibited by modifying energy spread and rms length.

However, in addition to these average effects, experiments demonstrate nontrivial dynamics above the threshold, where bunch oscillates periodically in relaxation oscillations. (Similar phenomenon in plasma has been studied before by O'Neil). In the SLAC damping ring, where this instability has been studied in detail, the rms length changed with time in a saw-tooth like fashion giving the name of the instability. Fig. 3a presents recent results obtained by B. Podobedov and R. Siemann in the damping ring.

Several models were suggested to explain this kind of behavior [10] [11] and it was reproduced in simulation [12] for some set of parameters. Dyachkov and Baartman [10]

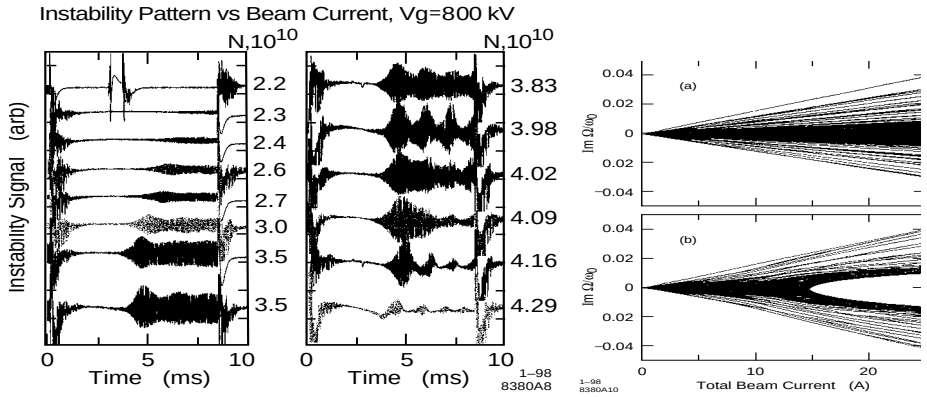

Figure 3: a) Saw-tooth instability in the SLAC NDR. Courtesy of B. Podobedov and R. Siemann. b) Growth rate of coupled-bunch modes without (upper plot) and with mode coupling [9]

assumed that PWD is strong enough to make potential with two minima. Initially, particles fill only the first minima, but diffuse later to the second minima due to quantum fluctuations. As a result, the self-consistent potential well changes and two minima merge. Filamentation and radiation cools the system to original state, and process repeats again The quasi-linear theory [13] [14], [11] describes effect of an unstable mode on the particle distribution in a self-consistent way. There are two possibilities. In one of them, the result is a steady-state distribution in the frame rotating with mode frequency, which corresponds to stationary nonlinear Van-Kampen waves in plasma. Another possibility, that unstable mode affects particles as an external perturbation. It traps particles in a separatix when amplitude is small, but separatrix shrinks at large amplitudes releasing particles. Situation here is similar to the situation wich takes place at the crossing of the nonlinear resonance with detuning.

This picture was supported recently by measurements of the beam transfer function (BTF) in the SLAC DR and at ALS [15], Fig. 4. The BTF was measured applying periodic RF phase modulation. The transfer function displayed an amplitude dependent deep, which was explained as a result of the beam splitting in the phase plane between two separatrices with cancellation of the net dipole signal. Experiment also allowed to measure diffusion rate between islands and associate it with Touschek effect.

Interesting results were obtained recently by Sebek and Limborg at SPEAR. They observed longitudinal saw-tooth oscillations of the amplitude of the upper side-band (around fundamental frequency).

However, the longitudinal single bunch dynamics is still not fully understood. Probably, different mechanisms of instability are possible depending on machine parameters, damping time, and current.

The single bunch transverse stability is defined mostly by mode coupling instability and head-tail effect. Both effects are not limiting factors for B-factories.

It is worth mentioning that new code TRISIM can be useful for single bunch simulation [16].

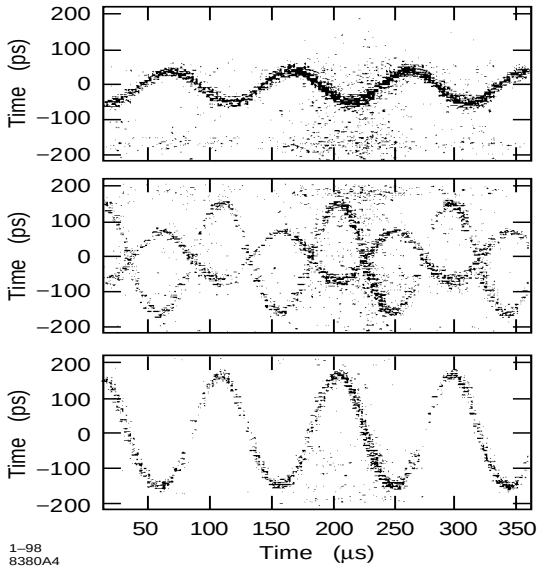

Figure 4: Streak camera observation of the beam split [15]

2.2 Multi-bunch Stability

Results on multi bunch stability in the case of equidistant bunches are well known and give simple way to predict longitudinal and transverse multi-bunch instabilities [17].

Mode coupling may substantially increase the growth rate of multi-bunch transverse oscillations above mode coupling threshold [9], see Fig. 3b. This results are especially important for quadrupole instability which is not cured by the present feedbacks.

2.2.1 Structure of the Eigen Modes

In the linear approximation, a beam is described by a well-known system of linear equation and stability of the system is an eigen-value problem. However, bunch pattern in the train in the new machines will not be equidistant. A gap is required to avoid ion trapping. It is known also that asymmetry in bunch population and/or in bunch spacing can stabilize beam. Some machines like SR for next linear colliders may use a number of trains of closely spaced bunches. Experiments at APS, Argonne [18] clearly showed dependence of the CB longitudinal instability on fill pattern and on the length of the train. A single rf HOM was found responsible for instability. It was shown that a single additional bunch could stabilize or destabilize the beam.

For an arbitrary fill pattern of bunches, the eigen-modes can be found solving the linear system. The beam spectrum can be very different from the spectrum of the equidistant bunches, see Fig. 5.

For a small gap, the structure of eigen modes can be found by perturbation theory, starting with the solution for equidistant bunches. The formalism is the same as in the time-independent perturbation theory in quantum mechanics. This cannot be valid for all modes simply because the number of modes M is smaller than the number of modes for the case of the equidistant bunches M_{eq}. It means, that for some modes the perturbation

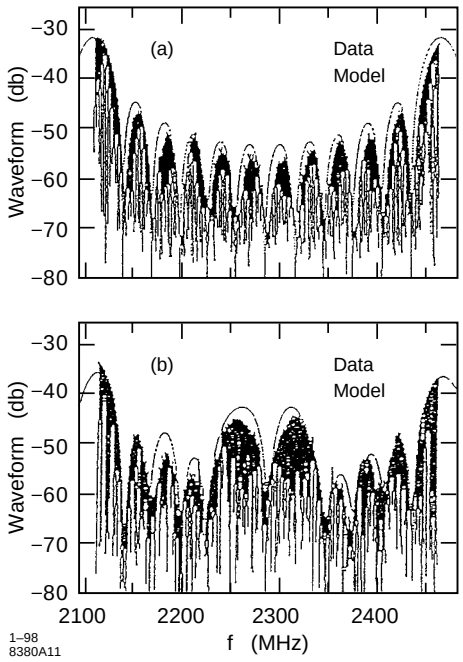

Figure 5: Spectra for stable (above) and unstable motion (below) of 4 trains with 12 bunches in each train [18]. Harmonic number $h = 1296$.

theory is not applicable. These modes are degenerate with approximately equal eigenvalues. The number of such modes is small. They can be selected and the system of equations for the subset of these modes can be solved exactly. The solution gives linear combinations of the degenerate eigen functions, which have to be used in the perturbation theory for non-degenerate eigen modes. The problem with different number of modes is eliminated in this way because the number of degenerate modes is $(M_{eq} - M)$.

For large gaps, the situation can be quite different. In all new machines, HOMs in rf cavities are damped and have low Q factors of the order of few hundreds. For gaps with the length $L_g = n_g s_b$ m, HOM wakes can become exponentially small across the gap provided $L_g/(2\pi R) > (Q/\pi)(f_0/f_{HOM})$, e.g. for PEP-II for a gap longer than 1% of the circumference, for 1 GHz HOM with $Q = 200$. Criteria when these wakes become negligible can be obtained on the basis of perturbation theory described above. The frequency shift of a bunch in the head of the train, due to the wake across the gap, should be compared to the bunch frequency spread in the beam, which is of the order of the growth rate of CB instability for equidistant bunches. The last has to be of the same order or larger than the radiation damping time for unstable CB modes.

At least in some cases the first bunch in a train does not see any wake. This is enough to make the system of equation degenerate and the analysis of CB motion in terms of eigen-modes is invalid [19]. Consider a simple daisy-chain case where a bunch is coupled only to the previous neighbor in the train with a constant wake W. For a large gap, it is simpler to consider the problem in the time domain. The first bunch does not see any wakes and oscillate with unperturbed synchrotron frequency ω_s. It drives oscillations of

the second bunch in the train but, because of the wake, the frequency of the second bunch is shifted by $\zeta \equiv \Delta\omega = W/2\omega_s$ and there is no resonance. (For the wake which have longer span, this would be true for all bunches within the span. Hence, situation in the head of the train is harmless). For the daisy chain, the frequency shift of the third bunch is the same as for the second bunch, and oscillations of the second bunch with amplitude a_2 lead to the resonant linear growth of the amplitude of the third bunch. The main term describing the motion of the n-th bunch is

$$y_n(t) = a_2 \frac{(-i\zeta t)^{n-2}}{(n-2)!} e^{i\omega_s[t+(n-2)s_b/c]} e^{-(\gamma_d/2)[t+(n-2)s_b/c]}. \tag{6}$$

At a given moment t, a bunch number $n_0 = \zeta t$ has the maximum amplitude. For this bunch,

$$y_{m0}(t) = i a_2 \frac{1}{\sqrt{2\pi\zeta t}} e^{[\zeta-(\gamma_d/2)]t} e^{i(\omega_s t - \pi\zeta/2)t}. \tag{7}$$

The beam is damped if $\zeta < \gamma_d/2$, exactly as in the case of equidistant bunches. However, the behavior is quite different, see Fig. 6. Bunch number n reaches maximum amplitude at time $t_n = 2n/\gamma_d$, different for different bunches, and then its amplitude exponentially decays. This transient behavior is a particular case of the so-called convective instability [20], contrary to the absolute instability of the closed train of bunches where all bunches grow in time simultaneously. Excitations of the beam can be driven by any of the bunches, leading to oscillations of the downstream bunches proportional to the amplitude a_m of the driving bunch. Each such an excitation can be considered as an analog to a coupled bunch mode.

2.2.2 Damping and Saturation of CB Instabilities

There are four main sources of damping: radiation damping, damping due to feedback systems, incoherent frequency spread (Landau damping), and damping introduced by the head-tail effect:

$$\frac{1}{c_0 \tau_{HT}} = \frac{e I^{av}_{bunch} |Z_\perp|}{E} \frac{RQ_\perp}{4\sqrt{2}\sigma_b} \frac{\omega_\xi}{\omega_0}. \tag{8}$$

Here ξ is relative chromaticity, and $\omega_\xi = (\xi/\alpha)\omega_\perp$ is chromatic frequency.

A reasonable estimate of Landau damping is given by the incoherent spread of frequencies. Frequency spread is introduced by PWD for quadrupole and higher order modes, and by by amplitude dependence of the tune for dipole transverse oscillations. Additional tune spread is given by beam-beam interaction and ions.

For example, for PEP-II [21], the second order effect of sextupoles give amplitude dependence of the tune $\delta\nu_x = a\epsilon_x + b\epsilon_y$, $\delta\nu_y = b\epsilon_x + c\epsilon_y$, with $a = -70$, $b = -871$ $c = -30$ $1/m$. and emittances $\epsilon_x = 49.2$ nm, $\epsilon_y = 1.48$ nm, the tune spread is 3.67 10^{-3} and 42.8 10^{-3} in x- and y-planes respectively. This can suppress coherent instability with growth time larger than 21 ms in y-plane, comparable with the SR damping time. In x-plane, though, it is only 318 ms.

Landau damping was revised recently [22] including tune spread in two transverse planes simultaneously, which improves stability. It was shown also that Landau damping is less effective for collimated beam with chopped off tails of the distribution.

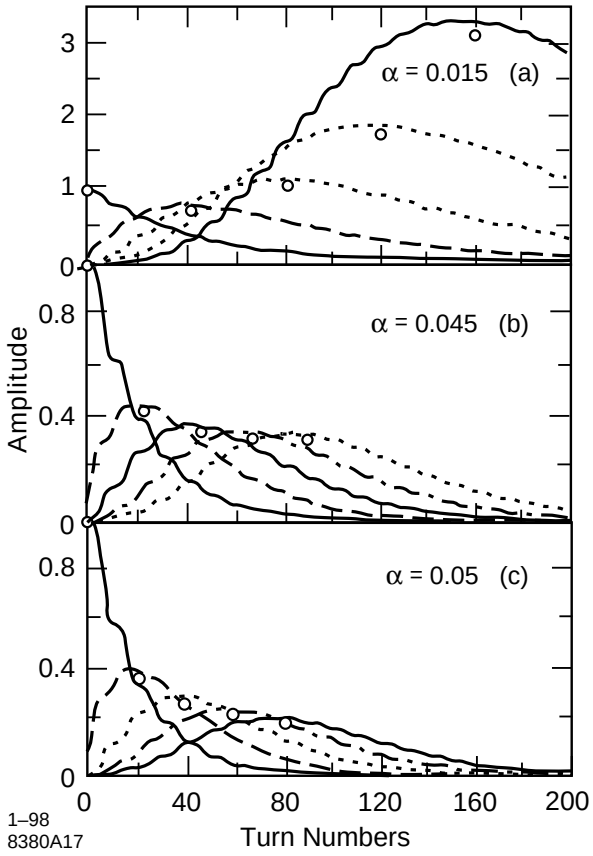

Figure 6: Transients in the train with large gap [19].

When the damping rate γ_d is small compared to the growth rate, the amplitude of oscillations increases but usually saturates at some limit [23], Fig. 7.

For a single bunch and for an impedance dominated by one HOM, the equation for the amplitude has the following structure:

$$\dot{A} = -\frac{\gamma_d}{2}A + \frac{\gamma_g}{\kappa\omega_s}J_1[\kappa\omega_s A]. \tag{9}$$

In linear approximation, the Bessel function can be replaced by its argument. This gives the result of the linear theory with growth rate γ_g.

For large amplitudes, there is another solution with the amplitude going to a constant [24]

$$A(\infty) = \frac{4(\gamma_g - \gamma_d)}{\kappa\gamma_g\omega_s}. \tag{10}$$

at $\Delta\gamma t >> 1$. The amplitude at saturation is very large for a single bunch. The situation, however, can be different for a train of bunches where ω_{HOM} can enter instead of ω_s.

Saturation was observed at ALS in qualitative agreement with theory. It was suggested by J. Byrd that because instability depends on the slope of the wake field at the bunch

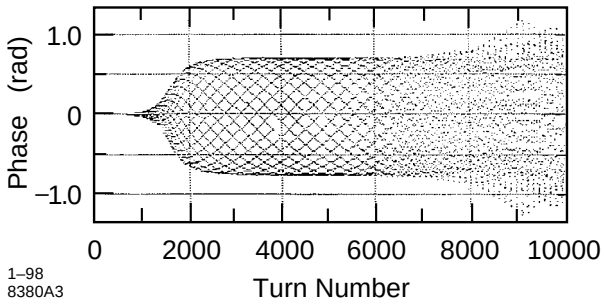

Figure 7: Saturation of coupled-bunch instability [23].

position, large longitudinal oscillations put bunch at locations with opposite slopes of the wake, averaging out its effect.

Experiments have also shown that large longitudinal oscillations can as well stabilize transverse instabilities. One mechanism is given by the dependence of the transverse kick $\Delta p_t^{\perp} = N_b e^2 W_{\perp}(s_l - s_t) x_l(s_l)$ on the distance between trailing (t) and leading (l) particles and works in the same way as for longitudinal motion. It is worth mentioning that the same reason may give synchro-betatron coupling for transverse motion which can be comparable with the coupling given by the dispersion in the rf cavities.

Another mechanism of stabilization of transverse motion is given by dependence of transverse beam spectra on amplitude of coherent longitudinal oscillations due to chromaticity. The amplitude of current spectrum of a particle in transverse case is proportional to $J_m[(n\omega_0 \pm \omega_\xi)A_s]$, where chromatic frequency $\omega_\xi = (\xi/\alpha)\omega_\perp$ is the ratio of relative chromaticity ξ to momentum compaction α, and A_s is the amplitude of synchrotron oscillations. For a beam with large amplitude of coherent synchrotron oscillations, saturation can be expected for amplitudes $A_s \propto \nu_m/|\omega_{HOM} - \omega_\xi|$, where ν_m is the first root $J_m(\nu_m) = 0$.For PEP-II, $\xi Q_\perp/\alpha \propto 10^4 \xi$ is comparable with $\omega_{HOM}/\omega_0 = 10^4$ for a typical HOM frequency 1.5 GHz at the moderate chromaticity of $\xi \propto 1$. It is worth noting that large chromaticity can reduce, however, the single particle dynamic aperture.

In nonlinear approximation, description of beam behavior in terms of modes may become meaningless for large machines even for equidistant bunches. The number of modes increases with number of bunches in the ring (or machine radius) while separation of mode frequencies depends mostly on the coupling of neighboring bunches and remains constant for a fixed bunch spacing. Hence, the mode density increases and, at some point, they may overlap, making beam behavior stochastic.

3 Stuffing Instabilities

A number of new instabilities has been discovered and studied extensively in the last years. Contrary to the classical instabilities driven by geometric impedance, these instabilities are caused by interaction with foreign (A. Chao terminology) particles like ions, dust, trapped- or photo-electrons. I call them stuffing instabilities. Actually, effect of ions and dust is hardly new and is well known for many years. The new fast Ion instability (FII)

is closely related to the two-stream instability and photo-electron instability has common features with beam induced multipactoring.

3.1 Effect of Ions

Ions produce tune shifts, increase tune spread, can cause transverse blow-up of a beam and reduce beam life-time. All these effects have been observed experimentally [25]. They are sensitive to vacuum, gap in the train, tune, and beam size. For example, Fig. 8a shows results for CERN EPA. For a single bunch in the ring, transverse emittances in both planes are independent on the bunch charge, while both emittances are strongly blown-up for multi-bunch beam at the same current per bunch. The dependence of the tune on bunch current $d\nu/dI$ changes sign from negative for a single bunch to positive for multi-bunch beam with the slope dependent on number of bunches in the train. The dependence on the number of bunches is also obvious for the life time. There was no emittance growth for the positron beam.

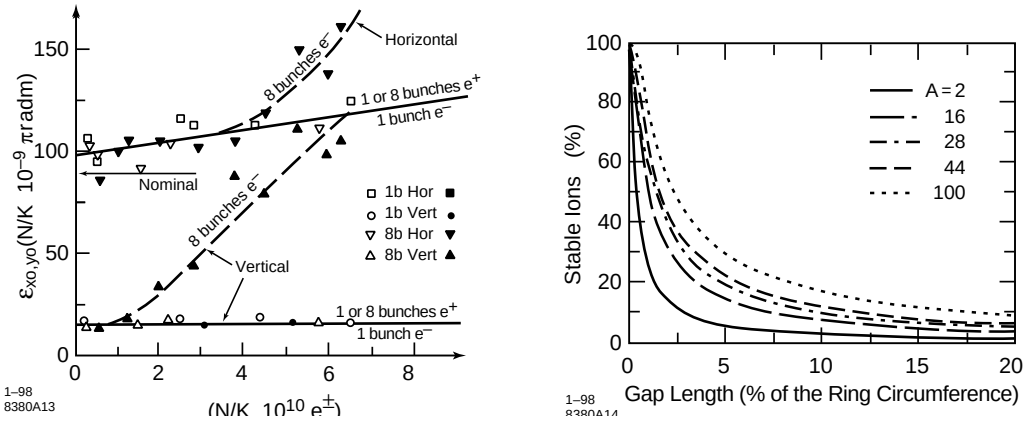

Figure 8: a) On the left: Effect of ion trapping on transverse emittance [25]. b)Percentage of stable ions in HER PEP-II vs gap length [26]

Ions are produced in collisions with residual gas at room temperature with the rate per electron given by

$$\frac{dN_i}{dt} = 300(\frac{p}{nTorr}) \sum g_k(\frac{\sigma_k}{Mbarn}) \quad \frac{1}{s}, \tag{11}$$

where the sum is over species in the ring, σ are ionization cross-section of a species, and g_k is percentage of the k-th species. For typical species, H_2, CO, CO_2, with atomic numbers $A = 2.\ 28,\ 44$, the cross-sections are $\sigma = 3.5,\ 1.9\ ,3.0$ Mbarn, $g = 0.75,\ 0.14,\ 0.07$, respectively. For high current machines, ionization by synchrotron radiation can give comparable rate [27].

Trapped ions oscillate in the average beam potential with frequency

$$\Omega_{x,y}^2 = \frac{eI_t Z_0}{2\pi A m_p \sigma_{x,y}(\sigma_x + \sigma_y)}. \tag{12}$$

For the total current in PEP-II $I_t = 1$ A, frequency are $\Omega_y/2\pi = 23.8/\sqrt{A}$ MHz, and $\Omega_y/2\pi = 10.6/\sqrt{A}$ MHz.

A train of equidistant bunches with bunch spacing s_b traps ions with atomic number $A > A_{th}$ if

$$|\cosh(\Omega_{sp} s_b/c) - \frac{\Omega^2 s_b}{2c\Omega_{sp}} \sinh(\Omega_{sp} s_b/c)| < 1, \tag{13}$$

where $\Omega_{sp}^2 = (4\pi r_p c_0^2/A) n_i$ describes the space-charge effect at the ion density n_i.

If the space-charge effect can be neglected, ions become unstable at the currents $\Omega\tau_b/2 > 1$. This gives the lowest atomic number of ions which can be trapped in a continuous train of bunches, with N_b electrons per bunch:

$$A_{th} = \frac{N_b r_p s_b}{2\sigma_x \sigma_y}. \tag{14}$$

For a train of equidistant bunches, the ion density increases in time and then saturates. There are several mechanisms of saturation: ion recombination, secondary ionization, beam driven diffusion, and two-stream instability. The first effect is very weak. The cross-sections of the first and secondary ionization are comparable, and this process gives saturation at the residual gas density $n_{gas} = 3.2\ (p/nTorr)\ 10^7\ cm^{-3}$ (at room temperature). Note, that the maximum ion density $n_i = n_{gas}$ can be lower than the neutralization density which is equal to average electron density in the beam $n_{neut} = N_b/(2\pi\sigma_x\sigma_y s_b)$. For PEP-II, $n_{neut} = 1.3\ 10^{10}\ cm^{-3}$. Beam driven diffusion can reduce the density at saturation even further by an order of magnitude.

A gap T_g in the train of bunches makes most ions unstable. Stability is very sensitive to small variations of the phase advance per turn $\phi = \Omega T_0$, and ions remain stable if the phase is within $n\pi < \phi < n\pi + 4/(T_g\Omega)$ for any integer n. Therefore, the variation of beam parameters along the ring leads to small zones of stability whose location changes in time with current and emittance. The distance between zones corresponds to variation of Ω by $\Delta\Omega/\Omega = \pi/(\Omega T_0)$. Some stable zones in both transverse planes overlap, giving zones of 2D stability. They are wider in the quads. Ions can escape from these zones due to the variation of the beam potential along the ring with variations of the β-functio [28]. Other effects leading to longitudinal motion are weaker.

If a stable 2D zone is at the center of a defocusing quad, ions may be stable longitudinally as well. Fig. 8b shows the percent of stable ions vs gap length for PEP-II [26]. 3D stable ions are accumulated until their space-charge shifts the ion frequency by $\delta\Omega/\Omega \propto 1/[(\Omega T_0)^2(\Delta T/T_0)]$. To addition to 3D stable ions, there are also ions, which are cleared in one turn but give, nevertheless, noticeable contribution.

The ion distribution is not Gaussian but Christmas-tree like [29]. This increases tune shift due to ions.

Attempts were made to reduce ion effects by exciting betatron oscillations of the beam at the ion frequency to drive ions to large amplitudes where their motion becomes stochastic due to nonlinearity of the beam potential. Although this shaking method can suppress effect of ions, it was found difficult to keep ions in resonance due to detuning at large ion amplitudes [30]. It should be noted that a gap in a bunch train also creates problems, exciting transients in rf cavities and making bunches in the head of the train different and vulnerable to the PACMAN effect. Transients are compensated in PEP-II by introducing

a partially filled gap also in the positron beam, to match bunch phase modulation in both rings. At injection, the width of stable zones, which scales as $\sigma_\perp/\sqrt{I_t}$, can be large and ion effects are most dangerous. Filling pattern of the train should be favored which preserve large gaps as long as possible. As the current decays, ions accumulated in 3D stable zones can become unstable. This may be the reason for dips in the life-time of decaying beams.

Ions produce a tune shift proportional to their total number in the ring N_i^{tot}:

$$\Delta\nu_y = -\frac{r_e N_i^{tot} < \beta_y >}{2\pi\gamma\sigma_y(\sigma_x + \sigma_y)}. \tag{15}$$

The horizontal tune shift has the same sign but is smaller by a factor σ_y/σ_x.

The single-turn ions give tune variation along a bunch train, linearly increasing toward the tail of the train. This has a positive effect by detuning bunches and suppressing coupled-bunch instabilities, including the fast ion instability.

Ions can also produce coupling between bunches, leading to a two-stream instability [31] at resonances $Q_y + \Omega_i/\omega_0 = integer > 0$. Effect was simulated for KEK PF [32]. At small amplitudes, the instability is very fast: the growth time can be of the order of a microsecond. In the steady-state, ions are driven to the wall by interaction with the beam while the beam remains transversely blown-up. An instability due to ion coupling was observed also in the SLAC electron storage ring [33]. The beam profile measured on the extracted beam was blown up for 2 bunches in the ring compared to a single bunch operation, (see Fig. 9). There was a large number of self-excited vertical betatron sidebands with sideband amplitudes oscillating with periodic bursts. The measured beam transfer function also agrees with coupled-oscillator model.

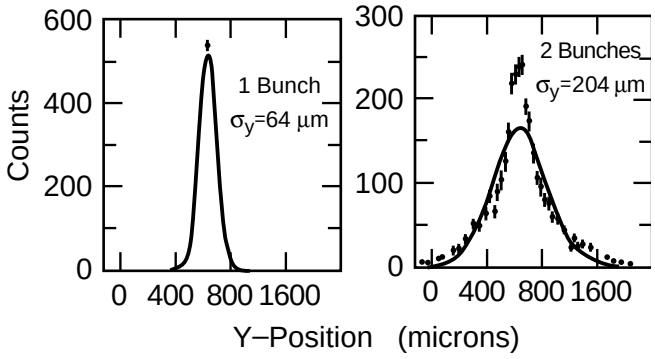

Figure 9: Two-stream instability at SLAC DR [33].

One-turn ions can give noticeable bunch coupling before ions move to large amplitudes. This coupling can cause instability for both electron and positron beams [34]. The growth rate of instability for positron beam is

$$\frac{1}{\tau} = \frac{2\eta}{\gamma}[(\frac{m_p}{m_e})\frac{N_t r_e A}{2\pi Q_y\sqrt{\epsilon_x\epsilon_y}}]^{1/2}, \tag{16}$$

where $\eta = n_{gas}\sigma^+ c_0$ is production rate of ions, $N_t = N_b M$ is total number of positrons in the beam, $\epsilon = \sigma^2/\beta$ are transverse emittances, and Q_y is betatron tune.

Ions can cause vacuum problems as was discovered at ISR over 20 years ago. Accelerated by the beam, they can hit beam pipe wall and release additional molecules which, when being ionized by the beam, produce run-away increase in pressure provided the secondary ion yield η_i is large:

$$\psi \tan \psi > \frac{S}{2W}, \quad \psi^2 = \eta_i \sigma^+ \frac{I^{av}_{beam}}{e} \frac{L}{4W}, \tag{17}$$

where W is pipe vacuum conductance (in litter/s), S pumping speed (litter/s), and σ^+ is the cross-section of ion production. The yield η_i, the number of outgased molecules per ion, increase with ion mass and energy, decreases with mass of outgased molecules, crucially depends on material of the wall and wall treatment, and can vary in the range from $\eta_i = 0.01$ to $\eta \simeq 10$. The best way to avoid instability is to use glow discharge treatment of the beam pipe and use titanium coating.

Machines with Al vacuum chambers like HERA and DORIS suffer from dust, macroparticles with atomic number, apparently released by the ion sputter pumps, and ionized and trapped by the beam. The life time is reduced by the breamsstrahlung. A macroparticle can have $N \propto 10^{12} - 10^{13}$ atoms and a radius of few microns. Dust causes sudden reduction of the electron beam lifetime at the threshold of about 10 mA (3 mA) at an energy 12 GeV (26.5 GeV), respectively. The life time shows a hysteresis behavior: it remains low even when the current is reduced below the threshold. Although replacement of a bad vacuum section improved situation, the problem remained. For PEP-II estimate [35] gives a thermal lifetime of trapped macroparticles less than 10 μs.

3.2 Fast Ion Instability

The Fast Ion Instability (FII)described by Raubenheimer and Zimmermann is driven by ion induced coupling between bunches. Mechanism is quite similar to the two-stream instability, but is driven by one-turn ions and therefore remains with a gap in the train. The instability does not have resonance character, although the growth rate depends on the length of a train. Similar effect can take place in positron machines and even in linacs due to trapping of electrons. The beam works as a noise amplifier magnifying oscillations of the first bunch along the train, although the last bunch does not necessarily have the largest transverse amplitude.

In the linear theory [36], the amplitude of the n-th bunch increases with time quasi-exponentially

$$a_n(t) \propto e^{\sqrt{t/t_c}}, \quad \frac{1}{c_0 t_c} = \kappa \frac{\Omega_i L^2}{2\omega_\perp}, \quad \kappa = \frac{4 r_e}{3\gamma s_b \sigma_x \sigma_y} \frac{dN_i}{ds}. \tag{18}$$

Here $dN_i/ds = 0.06(p/Torr)N_b\ 1/cm$ is the number of ions produced by a bunch with N_b electrons in one turn per cm, $L = M s_b$ is the length of the train, and $\omega_\perp = Q_\perp \omega_0$.

The characteristic time for PEP-II is $\tau_c = 5.5\ \mu s$ for 10 ntorr pressure of CO. Fortunately, spread of ion frequencies around the ring $\delta\omega_i$ makes situation much better [37]. The dependence on time becomes exponential, $a_n(t) \propto e^{-t/t_e}$ where, for the last bunch in the train, $\tau_e = \tau_c(2\delta\omega_i L/c_0)$. For PEP-II, $\tau_e = 350\ \mu s$ for 10% ion frequency variation around the ring and 760 μs for 30%. Variation of the ion frequency within a bunch has a smaller effect.

The beam has broad spectrum of betatron side-bands with an envelope centered at the ion frequency with lower sidebands having larger amplitudes than upper sidebands. The train profile is, in zero approximation, triangular with larger bunches at the end of the train.

The linear theory is not applicable at large amplitudes of oscillations. Numerical simulations show,(Fig. 10), that exponential growth is replaced by approximately linear time dependence. In the nonlinear regime, beam and ion centroids are separated by more than transverse rms $d > \sigma_y$ and, for Gaussian bunches, interaction is suppressed. Analysis shows [38] that, for flat beam and $\sigma_y << d << \sigma_x$ the interaction becomes a step-function, proportional to $d/|d|$. Such an interaction has a broad spectrum including the betatron frequency, which drives amplitude of a bunch linearly with time. For the last bunch,

$$A \propto \frac{\kappa L^2 \beta_y}{4\pi p_f} \frac{t}{T_0}, \tag{19}$$

where $p_f = L/(2\pi R)$ is the filling factor. The spectrum of a beam in the nonlinear regime moves toward lower frequencies due to blow-up of σ_y.

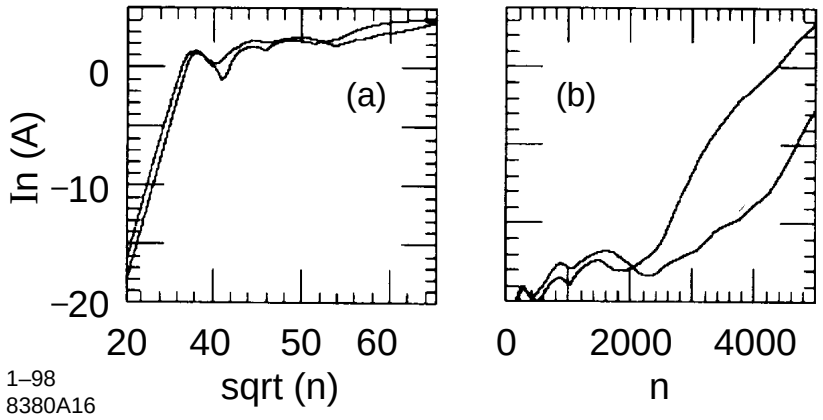

Figure 10: Amplitude growth due to FII vs number of turns. The linear growth is clearly seen in the logarithmic scale (in the left) but is replaced with linear growth later in time (usual scale, in the right).

In all formulas above, the amplitude of bunches were proportional to the amplitude of the first bunch. Any damping by radiation or feedback damps out oscillations of the first bunch. After that nothing drives oscillations of the following bunches and they vanish due to damping. With noise, however, it is possible to have a steady-state distribution within the train [39] [40]. There are several sources of noise: feedback systems, fluctuations of number of ions, and interference of perturbations introduced by different bunches. Because damping reduces the amplitude exponentially $a \propto e^{-t/\tau_d}$ while amplitude grows only linearly in time in the nonlinear regime, one can argue that equilibrium can be achieved only in the linear regime. With this assumption, the beam profile in a system with damping and random noise was found [39] to be dependent on the parameter $\eta = z\sqrt{\tau_d/\tau_c}$. If $\eta << 1$, the rms amplitude increases along the train as $< y^2(z) > \propto \eta^3$. However, for

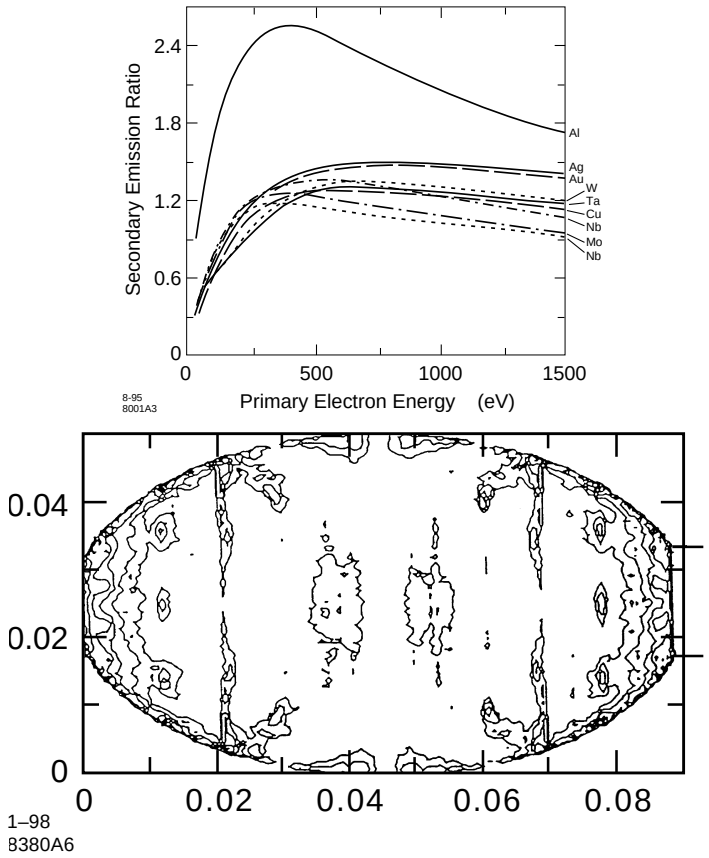

Figure 11: a)Above: Yield of the secondary electron emission. b) Below: Snapshot of the density of electron cloud [49].

$\eta > 1$, the growth along the train is exponential $< y(z) > \propto e\eta^2/2$. This behavior can be seen in simulations and experiments.

Beam spectra and transverse rms averaged over the train and for individual bunches were measured in experiments studying fast ion instability and carried out at ALS [41], TRISTAN AR at KEK, and PLS, Pohang [42]. In all cases, see Fig. 12 and 13, blow-up of the beam has been observed with saturation at 2-3 rms σ_y. Scaling of the effect with pressure and beam current, dependence on the transverse rms, and beam profiles were found to be consistent with theory. In saturation, the amplitude depends on the gain of the feedback system [43].

In most of the experiments, pressure was increased above nominal to enhance the effect. Additional to that, beam remains stable, and it may be to early to draw conclusion how detrimental it will be for operation. It may be possible, though, to control FII is by introduction of short gaps in the bunch train.

3.3 Electron Driven Instabilities

3.3.1 Beam Multipactoring

The first electron related instability was beam induced multipactoring instability at the ISR [44]. In the positron SR, electrons produced in the beam pipe with initial offset from the positron beam y can be accelerated to a velocity $v/c_0 = 2N_b r_e/\gamma y$ and, hitting the wall, produce secondary, low-energy electrons. The yield η_e of the secondary electron emission varies but can be as high as several units, Fig. 11a. The lowest yield is for Cu chamber, the highest, $\eta_e = 2.5$ is for Al at the primary electron energy 400 eV. It goes for Al below one for electrons with energy less than 50 eV and above 2.6 keV. TiN coating can reduce the yield to $\eta_e \simeq 1$. Effect depends on beam current, bunch spacing s_b, and the beam pipe radius b.

At the threshold current $\xi = N_b(r_e s_b)/b^2 > 1$ electrons reach the wall and produce secondaries before the next bunch arrives. If diffusion and loss of the secondaries to the wall are small, they will be accelerated by the next positron bunch and, for $\eta_e > 1$ may start avalanche. For PEP-II parameters, that may happen only at the currents more then 3A, substantially higher than the nominal current. The same is true for DAΦNE.

At lower currents, electron may experience several kicks from the bunches before they reach the wall. A similar situation takes place in dipoles where electrons spiral around B-field lines and move slowly in the vertical direction. For example, electrons reach the wall at the moment the second bunch arrives, at a current $\xi[1 + 1/(1 - \xi)] = 2$. However, the space charge effect may wipe this resonance out. Resonances at lower currents are even less probable because the electron trajectories begin to resemble random walk, and are susceptible to small perturbations.

Multipactoring electrons may also ionize the residual gas what affects pressure instability increasing effective production rate of ions. Estimates show that the effect is small.

3.3.2 Trapped Electron Instability

An electron related instability was causing a horizontal multi-bunch instability (mainly of the positron beam) at Cornell. It had a strong nonlinear dependence of the growth rate on current, and was present only when the distributed ion pumps were powered with dc voltage. This instability is due to the beam interacting with electrons [45] produced by synchrotron radiation in the beam pipe. Electrons are trapped by the combined magnetic field of the dipoles and the electrostatic field of the DIPs, which leaks into the vacuum chamber through pumping slots. Electrons are ejected by beam passage and the variation of the density transfers information on bunch displacement to the following bunches.

Similar effects can be produced by electrons trapped in the combined magnetic field of dipoles and the average electric field of the beam [46]. At the nominal parameters of the PEP-II LER, the positron beam can produce a potential well with a depth of the order of 100 eV. Electrons with such energy oscillate vertically, spiraling along magnetic field lines with a very small Larmor radius about 20 μm. Kicks from the bunches make electrons close to the beam unstable. The maximum density of the electrons is reached at about 1 cm from the beam. Electrons are produced, as in Cornell, by synchrotron radiation and can be accumulated with time provided the beam does not have a gap.

3.3.3 Photo Electron Instability

A coupled-bunch instability caused by photo-electrons (PE) was observed in KEK-PF positron ring [47] and recently studied by IHEP-KEK collaboration in BEPC, Beijing [48].

The main features of the instability is low threshold current (15-20 mA), broad distribution of betatron sidebands, and dependence of the threshold on bunch spacing. This instability does not occur in an electron beam. The growth rate of the instability can be very high. Simulations predict growth times of the order of 0.1 ms for KEK B-factory, 0.3 ms for PEP-II [49], and 0.5 ms at BEPC. In the BEPC experiments, the threshold of instability was 9.4 mA for 158 positron bunches, where vertical betatron side-bands were excited. The threshold current in the Beijing experiments depended on vertical chromaticity, and was increased by a factor of four when bunch spacing was doubled. The dependence on chromaticity is mostly due to Landau damping due to increasing amplitude dependence of the tune at large ($\xi_y > 8$) vertical chromaticity [50].

The photo-electron instability was explained by Ohmi [51]. Photo-electrons (PE) are produced by photo emission induced in the beam pipe walls by synchrotron radiation. They produce bunch-to-bunch coupling. Two basic mechanisms of coupling are possible: due to primary PEs and due to electron cloud build-up in the vacuum chamber in a steady-state operation.

The photons come to the wall at about the same time when the parent bunch passes by. The delay $\delta l \simeq b\sqrt{b/2\rho}$ is small compared to the bunch length. If the reflectivity of the wall is low, the primary PE are produced between the distances s_{min}, defined by the wall work function, and s_{max}, defined by the length of dipoles and the bend radius. The energy of primary photo-electrons is low, of the order of 5 to 10 eV, but emitted electrons see the electric field of the parent bunch and can be accelerated to 100-200 eV depending on the beam current and beam pipe geometry. Electrons emitted by photons from the head of the bunch get the largest kick, while those due to radiation from the tail remain at the wall. Because the electric field lines are normal to the wall, photoelectrons are accelerated in the horizontal plane, making a strip with the length increasing in time to Δx at the moment when the next bunch arrives. The density of the strip depends on the bunch current, the yield $\eta_{e\gamma}$ of electron emission, and the geometry of the beam pipe. The PEP-II ante-chamber, with the vertical opening $h_g = 1.5$ cm, substantially reduces this density. At 3A total current and for $\eta_{e\gamma} = 0.1$, the density in the strip is of the order of $n_{e\gamma} = 3.6\ 10^5\ cm^{-3}$.

The strip has vertical offset equal to the offset y_l of the parent bunch, and, hence, a kick to the incoming bunch from the strip depends on this offset as well. Retaining only the term proportional to y_c, the beam motion is described by the equation [52]

$$y'' + k_\beta^2 y = -\lambda y_l, \quad \lambda = 8\pi\eta_\gamma\eta e\gamma \frac{N_b r_e b}{\gamma s_{max} h_g^2 \Delta x} \ln\frac{s_{max}}{s_{min}}, \tag{20}$$

where $\eta_\gamma = 4\ 10^{-3}$. Oscillations of the first bunch are amplified by the following bunches. For PEP-II parameters, the amplitude of the second bunch grows and becomes equal to the amplitude of the driving bunch in 0.7 ms.

This simple mechanism works in the straight sections. Generally, it competes with more complicated processes of building up an electron cloud, Fig. 11b, with interaction of bunches through excitation of the cloud in a way very similar to the Cornell instability.

In this case, the situation is very similar to the multipactoring situation below the single-bunch threshold. Note that the interaction with the electron cloud gives a kick to an offset bunch even if all bunches ahead are not displaced. This self-induced kick gives a tune shift which depends on the density of electron cloud. For a train of bunches with a large gap, this mechanism can lead to detuning of bunches along the train stabilizing the beam. The equilibrium density of the cloud depends on many factors such as yield η_e of the secondary electron emission, wall reflectivity, and shape and roughness of the beam pipe. The electrons of the cloud kicked by the beam to the energy $2.6\ keV > E_e > 50\ eV$, can go to the walls and produce secondary electrons. The flux of the secondary electrons is added to the flux of primary PE and is balanced by losses of low energy electrons and the space charge effect of the cloud. Multipactoring can become a problem, especially in dipoles, where spiraling electron have larger η_e due to small incident angle. A short gap in the train $L_g > b\sqrt{mc^2/2E_\eta}$ leave only electrons with energy below $E\eta = 50$ eV which can not produce secondaries.

Consider a steady-state, where the average total potential of the beam and of electron cloud is at the level needed to stop secondary electrons with energy $E_e \simeq 5$ eV from entering the beam pipe. Such a consideration gives a density of the cloud of the same order as neutralization density $n_n = N_b/(\pi b^2 s_b)$, $n_n \simeq 10^7\ cm^{-3}$. The actual density is much lower and is defined by the dynamic equilibrium. Electrons which are at the distance r from the beam get a kick and can reach the wall before the next bunch arrives provided $r/b < -(1/2)[1+\sqrt{1+2N_b r_e s_b/b^2}]$. For currents $N_b r_e s_b/b^2 > 1$ this means that all electrons in the cloud hit the wall. For PEP-II, this parameters is 0.36 at 3A total current. The equilibrium is reached when the flux of electrons to the wall is equal to the flux of PEs $Q_{e\gamma} = \eta_{e\gamma} N_b dN_\gamma/ds$, where dN_γ/ds is number of photons producing PEs per unit length. For a beam pipe with ante-chamber, it is defined in [52]. If, however, the secondary yield $\eta_e > 1$ as for an uncoated Al chamber, the density of the cloud increases until it is stopped by space-charge effect.

Information on the bunch offset can be transfered to the following bunches due to a difference in the number of electrons in the cloud on both sides of the beam, and due to energy dependence of the yield η_e.

All these processes, experimental data on parameters, and realistic geometry are included today in simulations by K. Ohmi, M. Furman, and F. Zimmermann.

A relatively slow instability is expected at PEP-II, and the transverse feedback will be enough to cure it. TiN coating of the beam pipe (PEP-II), and a solenoidal magnetic field of 30 Gauss (KEKB) were suggested. Solenoidal field could add problems, because confined electrons may couple bunches as at Cornell, even if their density is hollow at the beam axis. Short gaps can prevent the equilibrium density to build up.

The study of the instability is still in progress. For example, an additional problem was pointed out recently [53] that due to vertical oscillations of a beam, a beam pipe wall would be irradiated which was not under synchrotron radiation of a quiet beam. This can enhance electron emission and induce transverse instability. The PEI today is maybe one of the main concern for beam stability in positron rings.

4 Conclusion

The new generation of machines push parameters of storage rings to a level never achieved before. A careful study of classical and new instabilities is necessary to reach the design goals. This is a challenging and exciting enterprise.

5 Acknowledgement

I thank A. Chao and L. Palumbo who encouraged me to write this paper and B. Zotter for his help.

References

[1] S. Kurennoy, Beam Coupling Impedances of obstacles protruding into beam, 1997 PAC, Vancouver, BC, Canada, 1997

[2] K. Yokoya Impedance of slowly tapered structures,a CERN SL/90-88 (AP) 1990,

R.L. Warnock A Formula For The High Frequency Longitudinal Impedance Of A Tube With Smoothly VArying Radius, SLAC-PUB-6191, April 1993,

G.V. Stupakov Geometrical Wake of a smooth Flat Collimator, SLAC-PUB-7167, May 1996

[3] G. Stupakov, S. Kurennoy, Trapped Electromagnetic Modes in a Waveguide With a Small Discontinuety, SSCL-Preprint-459, June 1993

[4] G.V. Stupakov Coupling Impedance Of a Long Slot and an Array of Slots in a Circular Vacuum Chamber, SLAC-PUB-6698, December 1994

[5] S. Heifets, SLAC-PUB-6122, April 1993. This approach was first considered by A. V. Novokhatsky

[6] R.D. Kohaupt, Longitudinal and Transverse Single Bunch Instabilities Induced By orbit Dependent HOM Losses, DESY 85-059, June 1985

[7] J. Haissinski, Exact Longitudinal Equilibrium Distribution of Stored Electrons in the presence of Self-Fields, Nuovo Cimento 18B, 72, 1973

[8] K. Oide, A Mechanism of Longitudinal Single-Bunch Instability in Storage Rings, KEK Preprint 94-138, 1994

[9] J.S. Berg Transverse Multibunch Head-tail Mode Growth Rates in the PEP-II B-factory, PEP-II AP Note 95.16, July 1995

[10] R. Baartman and M. D'yachkov, Simulation of Sawtooth Instability. PAC 1995, Dallas, Texas, May 1995, IEEE 1996, 5,3119

[11] S. Heifets, AIP Conf. Proc. 405, Santa Barbara, p. 117-133,1996.

[12] G.V. Stupakov, B.N. Breizman, and M.S. Pekker, Nonlinear Dynamics of Single Bunch Instability in Accelerators, SLAC-PUB-7377, December 1996

[13] Chin, Yokoya

[14] J. Schonfeld, Ann. Phys. 160, 149, (1985),

R.E. Meller Ph.D. Thesis, Statistical Method for Nonlequilibrium Systems with Applications to Accelerator Beam Dynamics, Cornell, 1986,

S. Heifets, Microwave Instability Beyond Threshold, Physical Review E, 54, p. 2889, 1996

[15] J.M. Byrd, W.H. Cheng, F. Zimmermann, Nonlinear Longitudinal Beam Response Measurements in Electron Storage Rings, PAC, 1997

[16] S. A. Heifets and G. Sabbi, Single Bunch Stability in LER of PEP-II, SLAC/AP-104, June 1996

[17] A.W. Chao, Physics of Collective Beam Instabilities in High Energy Accelerators, John Wiley and Sons, Inc. 1993;

M.S. Zisman, S. Chattopadhyay, and J.J. Bisognano, ZAP User's Manual, LBL-21270, UC-28, December 1986;

N. Dikansky, D. Pestrikov, Physics of Intense Beams in Storage Rings, Nauka, 1989 (in Russian).

[18] K.C. Harkay, et al, Compensation of Longitudinal CB Instability in Advanced Photon Source Storage Ring, PAC 97,

K. Harkay, Longitudinal Instabilities in the APS storage Ring, Workshop on Multibunch Instabilities, KEK, July, 1997

[19] P. Morton, Transient Behavior of Coupled Bunch Motion, PEP-II Workshop, September 1997;

K.A. Thompson and R.D. Ruth, Transverse coupled-bunch Instabilities in Damping Rings of High-Energy Linear Colliders, Phys. Rev. D, V. 43, 9, p. 3049. May 1991;

H. Okamoto, Beam Breakup in Bunch Trains, CERN-SL/94-75 (AP), September 1994

[20] L.D. Landau and E.M. Lifshitz, Course of theoretical Physics, Volume 10, Physical Kinetics, p.268, Pergamon Press

[21] Yunhai Cai, private communication

[22] J.S. Berg, F. Ruggiero, Stability diagrams for Landau damping. PAC, Vancouver, May 1997

[23] J. Byrd, PEP-II Workshop, 1997, PAC95

[24] S. Krinsky, Saturation of a Longitudinal Instability Due to Nonlinearity of the Wake Field, 1985 PAC, Vancouver, British Columbia, May 1985

[25] S. Bartalucci, et all, Collective Effects in the LEP electron Positron Accumulator (EPA), CERN PS/87-39 March 1987

[26] D. Villevald, S. Heifets, Ion Trapping, PEP-II AP Note 18-93, 1993

[27] S. Heifets, J. Seeman, W. Stoeffl, Pressure Stability under a Pump Failure, PEP-II AP Note 95.01, January 1995.

[28] D. Sagan Some Aspects of the Longitudinal Motion of Ions in Electron Storage Rings, Nucl.Inst. and Methods in Physics, Research, A307 (1991)

[29] P.F. Tavares, Transverse Distribution of Ions Trapped in an Electron Beam, CERN-PS/92-55(LP), September 1992

[30] J.C. Lee. et all, Suppression of the Transverse Oscillation in the SRRC Storage Ring by RF Knockout Method, PAC 97, 1997

[31] D.G. Koshkarev and P.R. Zenkevich Particle Accelerator, 3, 1, 1972; D. Sagan and A. Temnykh, NIM A344, 459, (1994)

[32] K. Ohmi, Two Beam Instability due to Ion-e Beam Interaction, KEK Workshop on Multibunch Instabilities, June 1997

[33] P. Krejicik, et al, Ion Effects in the SLC Electron Damping Ring, PAC 1997, Vancouver, 1997

[34] D. Pestrikov, Collective Instabilities of Bunches Due to Uncaptured Ions, KEK Workshop on Multibunch Instabilities, KEK, 1997

[35] F. Zimmermann, Trapped Dust in HERA and Prospects for PEP-II, PEP-II AP NOte 8-94, May, 1994

[36] T. Raubenheimer, F. Zimmermann, Interaction of a Charged Particle Beam with Residual Gas Ions or Electrons, SLAC, January, 1995

[37] G. V. Stupakov, A Fast Beam-Ion Instability, Proceedings of the International Workshop on Collective Effects and Impedance for B-factories, CEIBA95, KEK Proceedings 96-6, August 1996.

[38] S. Heifets, Saturation of the Ion Induced Transverse Blow-up Instability, Proceedings of the International Workshop on Collective Effects and Impedance for B-factories, CEIBA95, KEK Proceedings 96-6, August 1996, SLAC-PUB-7411 January 1997

[39] A.W. Chao and G.V. Stupakov, Effect of Feedback and Noise on Fast Ion Instability, International Workshop on Collective Instabilities (MBI97) KEK, May 1997, SLAC-PUB-7607, July 1997

[40] S. Heifets, Effect of Noise and Damping on Fast Ion Instability, MB197, KEK, May 1997

[41] J. Byrd et al First Observations of a Fast Beam-Ion Instability, SLAC-PUB-7507, May 1997

[42] M. Kwon, Experimenatl Results on FII at the PLS, MBI97, KEK, May 1997

[43] Y. Funakoshi, FII and Ion Trapping Experiments at TRISTAN AR, Multibunch Mini-Workshop, SLAC, September 1997

[44] O. Grobner, 10th Int. Conf. on High Energy Accelerators, Protvino, July, 1997

[45] J.T. Rogers and T. Holmquist, Distributed Ion Pumps Related Transverse Instability in CESR, Proceedings of the International Workshop on Collective Effects and Impedance for B-factories, CEIBA95, KEK Proceedings 96-6, August 1996

[46] S. Heifets, Transverse Instability driven by Trapped Electrons, SLAC/AP-95-101, October 1995

[47] M. Isawa, Y. Sato, and T. Toyomasu, Phys. Rev. Lett. 75, 1526 (1995)

[48] Z.Y. Guo, et. al. Experimental Study on Beam-Photoelectron Interaction in BEPC, KEK Workshop 1997

[49] M. Furman, G. Lambertson, Electron Cloud Instability in PEP-II, PAC, Vacouver, 1997

[50] K. Ohmi, Cromaticity Dependence of a Coupled-Bunch Instability in BEPC, KEK Workshop, May 1997

[51] K. Ohmi, Phys. Rev. Lett, 75, 1526, (1995)

[52] S. Heifets, Study of an Instability of the PEP-II Positron Beam (Ohmi effect and Multipactoring), SLAC-PUB-95-6956, also in CEIBA95 Proceedings, November 1995

[53] A.V. Burov and N.S. Dikansky, Electron-Cloud Instabilities, KEK Workshop, 1997

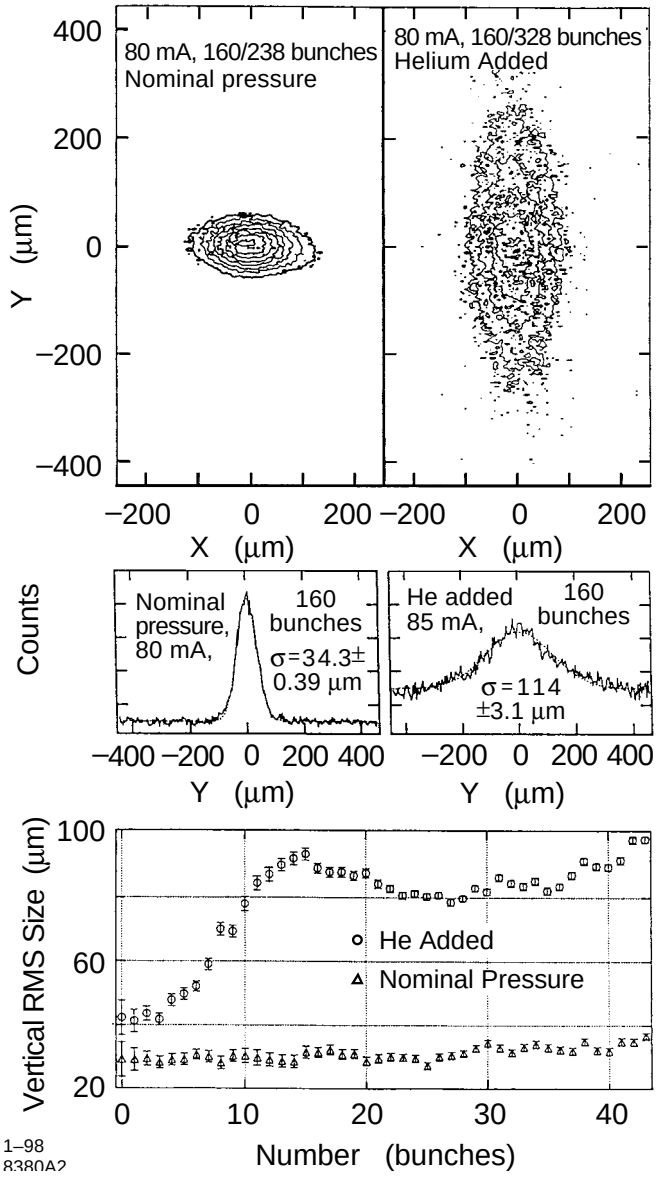

Figure 12: First results on FII [41].

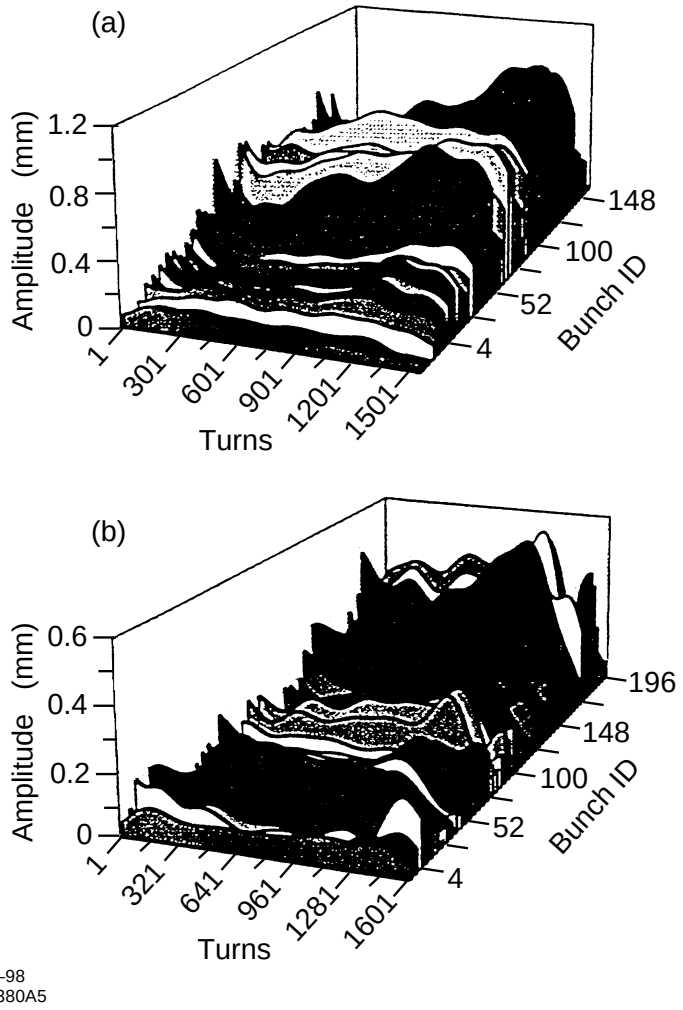

Figure 13: Beam profile in FII [43].